

Development of Diamond Schottky Barrier Diode

Natsuo TATSUMI*, Kazuhiro IKEDA, Hitoshi UMEZAWA and Shinichi SHIKATA

Diamond is seen as one of the most promising semiconductor materials to be used for power devices because of its superior physical and electrical properties, such as wide band-gap, high breakdown electric field, high mobility and high thermal conductivity. Through the technology for growing low-defect diamond, the breakdown field of diamond Schottky barrier diode (SBD) has reached 3.1 MV/cm, which was higher than that of SiC SBD. Though the heat of power device is the biggest problem for conventional semiconductor materials, diamond SBD was found to have low reverse leak current, high forward current density (3000 A/cm²) and long-time stability (1500 hours at 400 °C) at high temperature. Diamond is the best semiconductor material for devices featuring both energy saving and high power-density. A new progress in crystal defect analysis of diamond was achieved by comparing X-ray topography, etch-pit mapping and diamond SBD characteristics. The correlation between mixed dislocations of diamond and SBD leak current was found for the first time. The possibility of the application of diamond to power devices will be discussed using these results.

1. Introduction

Diamond, which has excellent physical properties, is attractive for use in industrial applications. Because diamond is rated the highest for hardness and heat conductivity among all known materials, it is widely used for products such as abrasive grains, cutting tools, and heatsinks. Diamond also exhibits excellent transparency even in the ultraviolet range and can be applied to optical tools. Because diamond is composed of carbon atoms, it has a high biological affinity and is used in dental drills and surgical knives.

Since carbon is a group element in the periodic table just like Si and Ge, diamond can be used as a semiconductor. SiC and GaN that are recently being studied extensively as wide band-gap semiconductors have band gaps of 3.1 eV and 3.5 eV, respectively, while diamond has a wider band gap of 5.5 eV. Various figures-of-merit (FOM) have been proposed by E. O. Johnson,⁽¹⁾ B. J. Baliga⁽²⁾ and A. Q. Huang⁽³⁾ as evaluation indices of power device materials defined based on physical properties such as carrier mobility, breakdown voltage and thermal conductivity. In the case of Baliga's FOM, the values for Si and SiC are 1 and 630, respectively, while that for diamond is as high as 44000, which means that diamond is a much more suitable material for high power devices than conventional semiconductor materials.

As the technologies for growing and doping diamond substrates have been increasingly developed in recent years, many researchers developed diamond electronic devices. Since the earlier study of diamond Schottky barrier diode (SBD) by H. Shiomi et al.⁽⁴⁾ (Sumitomo Electric Industries, Ltd.), diamond SBD has been developed by D. J. Twitchen⁽⁵⁾, T. Teraji⁽⁶⁾, and S. J. Rashid⁽⁷⁾. After the success in n-type diamond doping, S. Koizumi et al.⁽⁸⁾ had succeeded in developing a pn diode. The research groups led by H. Kawarada⁽⁸⁾ and M. Kasu⁽¹⁰⁾ developed the diamond MISFET and MES respectively using non-doped, hydrogen terminated dia-

mond and achieved a cut-off frequency as high as 28 GHz. These devices were developed as high-frequency, high-power telecommunication devices. On the other hand, the National Institute of Advanced Industrial Science and Technology (AIST) has begun its research on diamond high power switching devices since 2004.

In 2005, Sumitomo Electric started a collaborative research on diamond SBD with AIST. Because the SBD structure is the most simple structure among various power devices, Sumitomo Electric selected SBD as the most suitable device in terms of providing feedback to the diamond crystallinity evaluation process.

In this paper, the authors explain about the diamond SBD developed in the collaborative research and also about the possibility of developing a device featuring both energy saving and high power density.

2. High Breakdown Voltage Characteristics of Diamond

The structure of a diamond SBD is very simple: To achieve high breakdown voltage, Schottky electrodes were deposited on a low boron-doped p- diamond layer to expand the depletion layer(**Fig. 1**). In order to make good ohmic contacts, Ti/Pt/Au ohmic electrodes were deposited on a highly boron-doped p+ diamond layer. Although the ideal diamond SBD structure is the vertical structure illustrated in **Fig. 1**, the structure employed in the collaborative research was pseudo-vertical for ease of diamond growth, in which p- and p+ layers were grown on an insulating Ib (100) diamond substrate (**Fig. 2**). **Figure 3** shows a photograph of the developed SBD device. Ohmic electrodes were deposited on the four corners of the substrate and the Schottky electrodes of various sizes were formed on the center area.

A diamond SBD ordinarily shows a rectifying behavior as is shown in **Fig. 4(A)**. In order to enable an SBD to

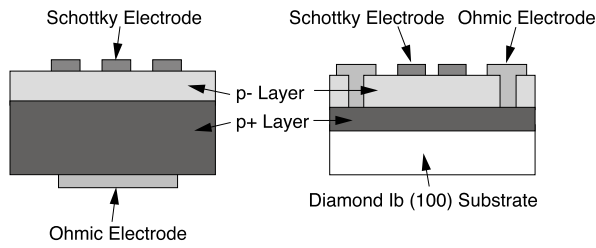


Fig. 1. Vertical SBD.

Fig. 2. Pseudo-vertical SBD.

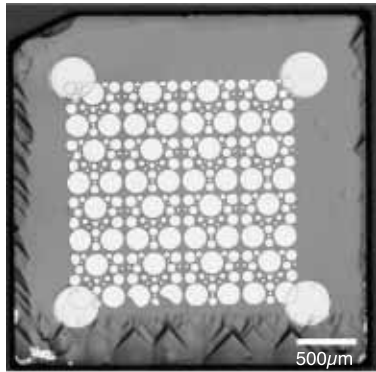


Fig. 3. Microscopic image of diamond SBD.

operate at high power, the sizes of Schottky electrodes need to be increased. When electrodes became larger than 100 μm in size, short circuit happened on the conventional diamond epitaxial layer as shown in **Fig. 4(B)**. The conventional epitaxial layer had such high quality that the mobility reached 1500 cm²/Vs and free-exciton luminescence could be observed by cathodoluminescence analysis. However, non-epitaxial crystallites existed on the diamond surface as seen in **Fig. 5**, and these crystallites caused short circuit problems. In order to increase operation current, the formation of non-epitaxial crystallites must be suppressed. Moreover, although thicker epitaxial layer could provide higher breakdown voltage, conventional growth speed was as low as 0.2 μm/h and it was difficult to grow thick epitaxial layer. To solve these problems, the authors investigated the effect of high microwave power and off-angle of the substrate on the suppression of crystallites and growth rate.

The off-angle of the diamond substrate was defined as shown in **Fig. 6(A)**. When a low microwave power of 0.8 kW was used, the density of non-epitaxial crystallites decreased as the off-angle increased, but the density did not become lower than 10⁴ cm⁻². On the contrary, when a high microwave power of 4.0 kW was used, the density of non-epitaxial crystallites rapidly decreased and no crystallites could be observed on a substrate with an off-angle larger than 2 degrees. Generally, step-flow growth of crystals occurs more easily on high off-angle substrates. In the case of step-flow growth of diamond crystals, the growth occurred easily in a high microwave-power plas-

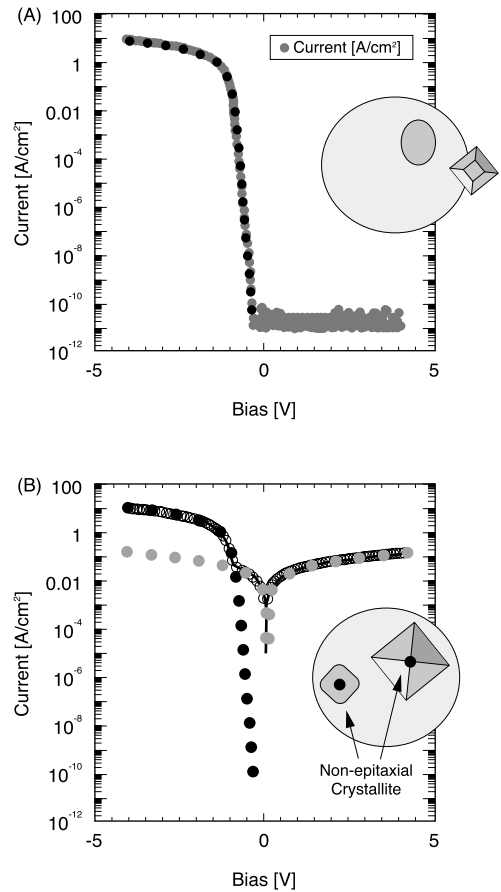


Fig. 4. I-V characteristics of diamond SBD. (A) Normal rectification property, (B) Short circuit caused by non-epitaxial crystallites in Schottky electrode.

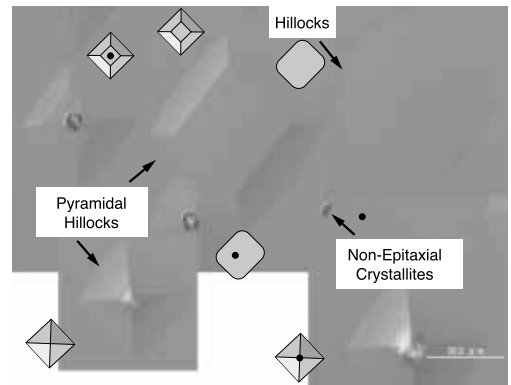


Fig. 5. Surface structure of conventional diamond epitaxial layer.

ma and non-epitaxial crystallites were wiped out by the flow of steps.

Next, the influence of off-direction was observed under the growth condition of 4 kW microwave power. When the off-directions of a diamond substrate were aligned to both <110> and <100>, the surface became very flat and no non-epitaxial crystallites were observed. However, when off-direction was between <110> and <100>, many large

hillocks grew and it was difficult to fabricate Schottky electrodes on the diamond surface. When off-direction was aligned to $\langle 110 \rangle$, the carbon atoms on the surface of diamond forms an orderly dimer structure (Fig. 7) and diamond grows easily by the step-flow mode. In this case, the surface of diamond was extremely flat and its roughness reached $Ra=1.1 \text{ \AA}$. The quality of this epitaxial layer was so high that the carrier mobility was as high as $1540 \text{ cm}^2/\text{Vs}$.

It was revealed from these results that high-quality diamond epitaxial layer without non-epitaxial crystallites can be grown by using high microwave power and a substrate with an off-angle larger than 2 degrees and an off-direction either $\langle 110 \rangle$ or $\langle 100 \rangle$.⁽¹²⁾

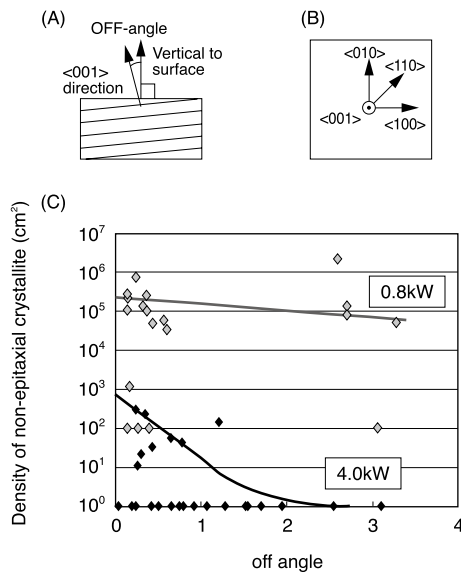


Fig. 6. Definition of off-angle, and relationship between non-epitaxial crystallite density and off-angle. Generation of non-epitaxial crystallites was suppressed by high off-angle and high microwave power. (A) Definition of off-angle (side-view), (B) definition of off-direction (top view), (C) graph of density of non-epitaxial crystallite vs off-angle.

Before the Schottky electrodes were formed on this diamond epitaxial layer, the surface preparation was needed to control the interface between the electrode and diamond. The surface of diamond becomes conductive when the surface atoms are terminated by hydrogen and becomes insulative when terminated by oxygen. The Schottky barrier height became low and the leakage current of the Schottky diode was high when the diamond surface was terminated by hydrogen. Therefore, diamond was terminated by oxygen by using oxygen radicals. After the oxidization treatment, Pt electrodes with Schottky barrier height of 2.0 eV were deposited. The reverse characteristics of the diamond SBD is shown in Fig.8. The breakdown field of diamond SBD reached 3.1 MV/cm ⁽¹³⁾, which was higher than 2.4 MV/cm of a SiC pn diode.

By carrying out the CVD method at a high microwave power, the growth rate was increased from 0.2 to 0.9 \mu m/h ,

enabling the growth of thick p- epitaxial layer. While the thickness of the epitaxial layers deposited using the conventional method was only 1 to 2 \mu m , the new fabricated Pt SBD had thickness of 14 \mu m and had a high breakdown voltage of 2.8 kV .

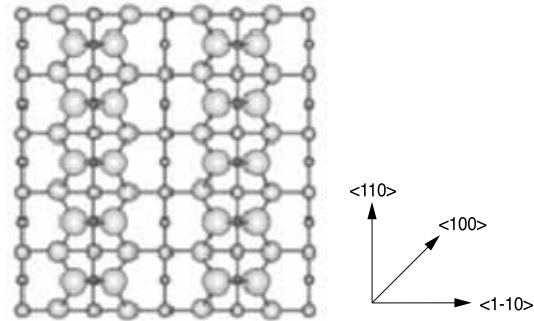


Fig. 7. Dimer structure of diamond surface atoms.

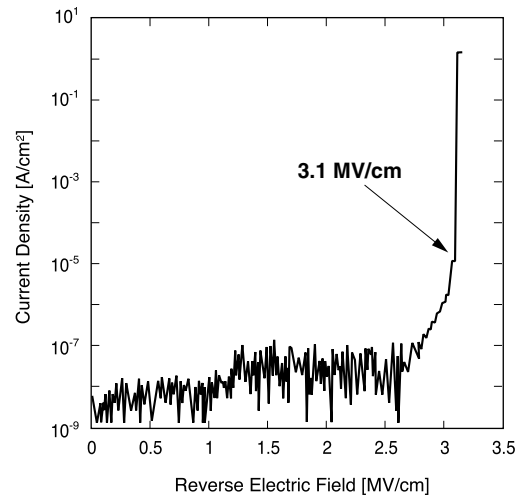


Fig. 8. Reverse characteristics of diamond SBD. Breakdown field of diamond reached 3.1 MV/cm , exceeding that of SiC.

3. Diamond SBD Characteristics at High Temperatures

Because wide band-gap semiconductor devices such as SiC and GaN devices have high breakdown voltage and energy-saving properties, use in high power applications such as hybrid vehicles and electric appliances are being expected. However, when high voltage and high current were applied to a device, excessive heat generation occurs and temperature becomes so high that it cannot be cooled by a cooling system. At room temperature, the reverse current is decided by the field emission mechanism in which the current tunnels through the Schottky barrier. At high temperatures, the thermal field

emission mode becomes dominant and not only the tunneling current but also carriers having heat energy pass over the Schottky barrier as a reverse leakage current. Therefore, the reverse characteristic of a diamond SBD in high temperature operation is determined based on not only breakdown voltage but also leakage current. The upper operation temperature limit of SiC SBD is 175 °C, which is higher than 125 °C of Si SBD. This is because the thermal conductivity of SiC (4.9 W/cmK) is higher than that of Si (1.5 W/cmK) and also SiC has wider band-gap and higher Schottky barrier height. These characteristics provide SiC with stable device operation at high temperature. GaN may allow low resistance and high breakdown voltage devices, but high power operation will be difficult to achieve because of its low thermal conductivity (1.3 W/cmK).

On the other hand, diamond has a thermal conductivity of 22.0 W/cmK, which is the highest value among all materials, and cooling is therefore not much of a problem any more. Because the band-gap of diamond is very wide, any electrode materials with high Schottky barrier height can be selected to create low leak-current, devices. **Figure 9** shows the reverse leakage current of SiC⁽¹⁴⁾ and diamond SBDs. The leakage current of a SiC SBD at room temperature was rather high, and that at 162 °C increased to 100 mA/cm² in an electric field of 1.5 MV/cm. The leakage current of the diamond SBD having Pt Schottky electrodes was below the measurement limit at room temperature and 0.1 mA/cm² at 142 °C, two orders lower than that of the SiC SBD at room temperature.⁽¹⁵⁾

High temperature also has a positive effect on the forward characteristics of the diamond SBD. Because impurity level is less than 63 meV for both Si or SiC,⁽¹⁶⁾ carriers are activated at a probability of almost 100% even at room temperature. However, as the temperature increases, the carrier mobility decreases, and conductivity decreases as a consequence. On the other hand, because diamond exhibits a rather high impurity level of 350 meV

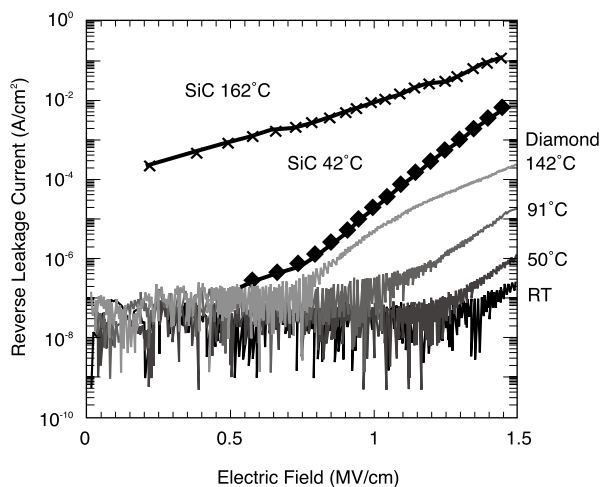


Fig. 9. Reverse leakage current of diamond and SiC SBDs⁽¹⁴⁾ at high temperatures. Leakage current of diamond SBD was smaller by 3 orders than that of SiC SBD.

for boron, although only a few carriers are activated at room temperature, more carriers are activated at higher temperatures. The maximum conductivity of diamond was achieved at temperatures around 100 to 200 °C, which are the upper operational-temperature limits for almost all other semiconductor materials. **Figure 10** shows the forward characteristics of the diamond SBD heated to 200 °C. The forward current density of diamond at 8 V reached 3000 A/cm², which was 3 times higher than the upper limit for SiC.⁽¹⁷⁾ Thus, diamond can be used to realize power devices that achieve both energy saving and extremely high power density.⁽¹⁸⁾

When power devices are operated in the high power condition, the long-term stability such as corrosion resistance of electrodes and semiconductors need to be considered. For this purpose, the diamond SBD was left in

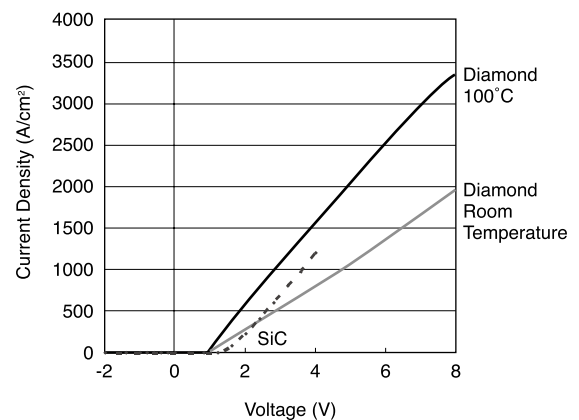


Fig. 10. High current-density operation of diamond SBD at high temperature. Highest current density reached 3000 A/cm², higher than 1000 A/cm² of SiC SBD.⁽¹⁷⁾

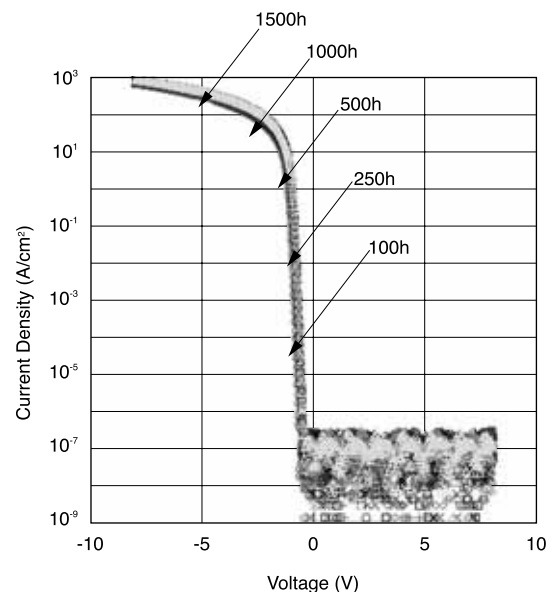


Fig. 11. Long-term stability test of diamond SBD. Characteristics did not change after 1500 hours at 400 °C.

400 °C and the change of SBD characteristics were observed (Fig. 11). With the Ru Schottky electrodes that are highly stable on the diamond surface, neither forward nor reverse characteristics of the diamond SBD changed even after 1500 hours. It was thus proven that diamond SBD is stable over a long term at high temperatures.⁽¹⁹⁾

These results show that diamond is the best material for realizing power devices featuring both energy saving and extremely high power density.

4. Crystal Defects and SBD Characteristics of Diamond

Detailed investigations had been made on the widely-used semiconductors such as Si and SiC regarding their crystal qualities and the influence the crystal defects have on device characteristics.⁽²⁰⁾ Crystal quality was also investigated for diamond, but investigations of diamond were made mainly on applications as abrasive tools or optical tools, and hardly any investigation was done on the relationship between diamond crystal defects and device characteristics. In this section, the authors report on the first study made on the relationship between diamond dislocation defects and device characteristics.

The authors used X-ray topography and the etch-pit mapping to observe diamond crystal defects. X-ray topography is a method for observing crystal perfection and defect distribution by capturing the distribution of X-ray diffraction intensity. The experimental setups for X-ray topography are shown in Fig. 12.

Dislocation is the displacement of atoms from their ideal crystal lattices (Fig. 13). This displacement vector (vector b) is called Burgers vector. The dislocation continues one-dimensionally until it reaches the surface or interface of the crystal. This direction is defined by line vector t . Basically, when vector b is parallel to vector t , the defect is called screw dislocation, and when vector b is perpendicular to vector t , the defect is called edge dislocation. In the real materials, the situation is more complicated that the angle between b and t can be 30 or 60 degrees and mixed-dislocation of screw and edge dislocations also existed. The intensity of dislocation image in X-ray topography (intensity I) is determined from the angle of diffraction vector g and Burgers vector b . The relationship can be described as $I = g \cdot b$. Intensity I reaches its maximum when vector g is parallel to vector b , and reaches its minimum when vector g is perpendicular to vector b . Based on this relational expression, the X-ray

topographic measurement using more than one vector g reveals the atomic structure of defects.

In this study, the X-ray experiment was conducted using synchrotron radiation at the High Energy Accelerator Research Organization. Synchrotron X-ray topography that provides extremely high definition images was performed at beam line BL15C. An FZ-Si (111) crystal monochromator was used, and energy resolution was 4 eV at an incident energy of 10 keV. X-ray topographic images were captured on a nuclear plate. First, an X-ray topographic image of the Ib (100) diamond substrate was captured. Then the diamond epitaxial layer was grown by microwave plasma CVD. Lastly, X-ray topographic image was captured again and the generation and propagation of dislocations were observed. Diffraction vectors $g = (113)$ and $g = (044)$ having a perpendicular components to the diamond surface and $g = (220)$ having a parallel components to the diamond surface were used for dislocation observation. The X-ray topography was conducted under conditions listed in Table 1.

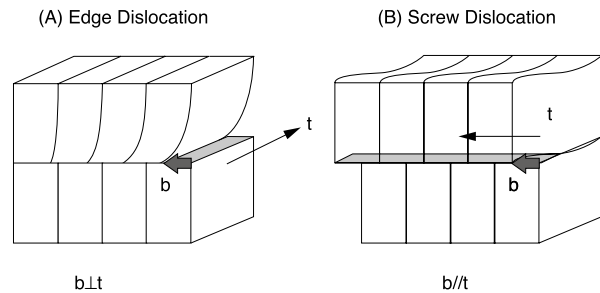


Fig. 13. Two types of dislocations and their Burgers vector b . Burgers vector b of edge dislocation is perpendicular to line vector t , while that of screw dislocation is parallel to line vector t . Image intensity I in X-ray topography depends upon relationship between Burgers vector and diffraction vector g .

Table 1. Conditions for X-ray topography.

Wavelength λ	0.96Å	0.91Å	0.71Å
Diffraction vector g	(113)	(044)	(220)
Incident angle ω	0.96	0.52	16.4
Diffraction angle 2θ	52.4	91.0	32.9
Angle of g to surface ψg	63.8	34.4	0

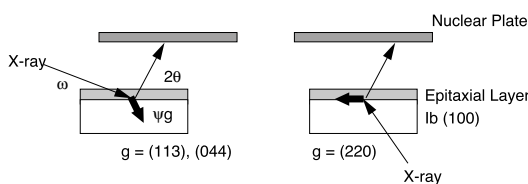


Fig. 12. Experimental setups for of X-ray topography

The X-ray topographic image of Ib (100) diamond substrate is shown in Fig. 14, on which many line- and dot-like dislocations were observed. The dislocations in the images of $g = (113)$ and $g = (044)$ were found at nearly the same locations. Few dislocations were seen in the image of $g = (220)$ and no obvious connections with other vector g images seemed to exist. This result indicates that most of the dislocations in this substrate were screw dislocations that have the Burgers vector and dislocation lines perpendicular to the substrate surface.

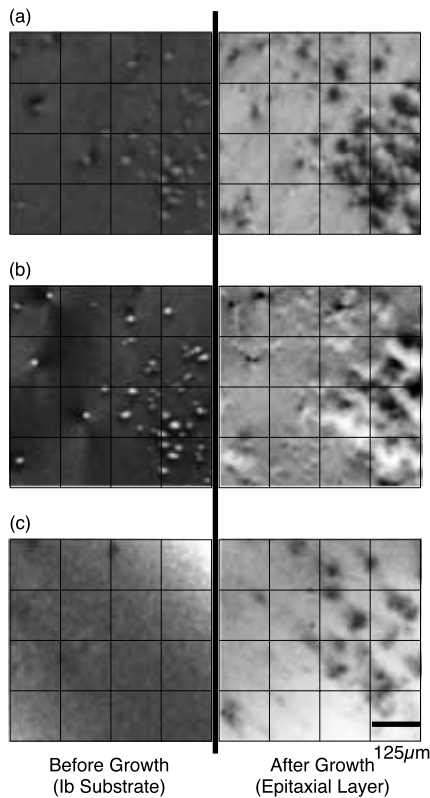


Fig. 14. X-ray topographic images of diamond substrate and epitaxial layer. Diffraction vectors were (a) $g = (113)$, (b) $g = (044)$ and (c) $g = (220)$. Dislocations increased after epitaxial growth. New mixed dislocations were generated in all images (a), (b) and (c).

After an epitaxial layer was grown, the dislocation density in X-ray topographic image increased drastically. While the dislocation density of the Ib substrate was $1.6 \times 10^4 \text{ cm}^{-2}$, that of the epitaxial layer was $2.8 \times 10^4 \text{ cm}^{-2}$. Dislocations in the Ib substrate were also seen after the epitaxial growth, and almost all the dislocations propagated to the epitaxial layer. The biggest difference between the epitaxial layer and the Ib substrate was dislocation density in the image of the diffraction vector $g = (220)$. While the dislocation density in the Ib substrate was as low as $1.6 \times 10^3 \text{ cm}^{-2}$, that of the epitaxial layer increased to $2.0 \times 10^4 \text{ cm}^{-2}$. Most of the dislocations seen in the image of $g = (220)$ in the epitaxial layer was also seen in the images of $g = (113)$ and $g = (044)$. Therefore, the Burgers vectors of increased dislocations in the images of $g = (220)$ were both perpendicular and parallel components to the surface, indicating that the dislocations that increased in the epitaxial layer were mixed-dislocations of screw and edge dislocations.

Then, to observe dislocations, etch pits were produced on the diamond using the microwave plasma etching method with a H_2/CO_2 gas mixture. **Figure 15** shows the microscopic images taken before and after the etching of the sample that had previously been observed by the X-ray topography. It is observed from this figure that etch-pits were produced only at some types of dislocations. The relationship between dislocations and etch pits are illustrated in **Fig. 16**. There were 4 types of dislocations in the

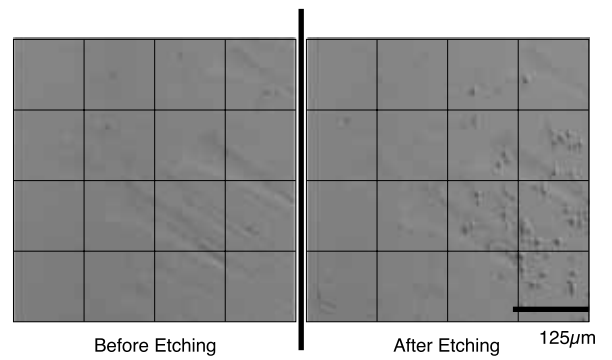


Fig. 15. Microscopic images of diamond surface before and after microwave plasma etching. After etching, etch pits were generated at areas where mixed dislocation images were observed by X-ray topography.

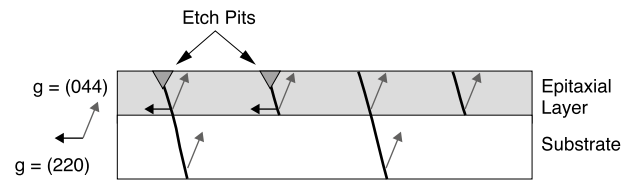


Fig. 16. Types of dislocations in diamond epitaxial layer. Thick lines represent dislocation propagations. Arrows represent directions of diffraction vector g by which X-ray topographic image of dislocation was captured. New dislocations were generated in epitaxial layer. All dislocations in substrate propagated to epitaxial layer and some of them changed into mixed dislocations. Etch pits were produced at mixed dislocations selectively.

sample. These dislocation types can be categorized according to whether dislocation propagated from Ib substrate to epitaxial layer or was newly generated, and also according to whether or not etch pit was formed. The dislocations without etch pits were simple screw dislocations whose images appear only with $g = (113)$ or (044) but not with $g = (220)$. On the other hand, the images of dislocations with etch pits were shown with all vectors $g = (113)$, (044) and (220) . These results indicate that the H_2/CO_2 microwave plasma selectively produced etch-pits only at mixed dislocations.⁽²¹⁾

Next, the relationship between SBD characteristics and crystal defects was investigated. After measuring the characteristics of the SBD having the quasi-vertical structure shown in **Fig. 2**, electrodes were removed by acid and etch pits were formed using the microwave plasma method. The microscopic images of etch pits and the plots of reverse characteristics of the diamond SBD are shown in **Fig. 17**. Larger leakage current is observed at electrodes with high etch-pit density than at those with lower etch-pit density. Because the atomic bonds in the mixed dislocations were different from the sp^3 structure in diamond, the depletion layer did not expand at this dislocation and it acted as a leakage path of reverse current.⁽²²⁾

Based on these results, by comparing the results of X-ray topography, microwave plasma etching and SBD characteristic measurement, the relationship between dia-

mond dislocation defects and device characteristics was found for the first time. This finding will enhance the development speed of diamond electronic devices.

6. Acknowledgement

The authors would like to gratefully thank Drs. T. Kato and H. Yamaguchi (Energy Semiconductor Electronics Research Laboratory, AIST) for their support and discussion in X-ray topography measurements.

The X-ray topographic imaging study using synchrotron radiation has been performed under the approval of the Photon Factory Program Advisory Committee (Proposal No. 2007G666).

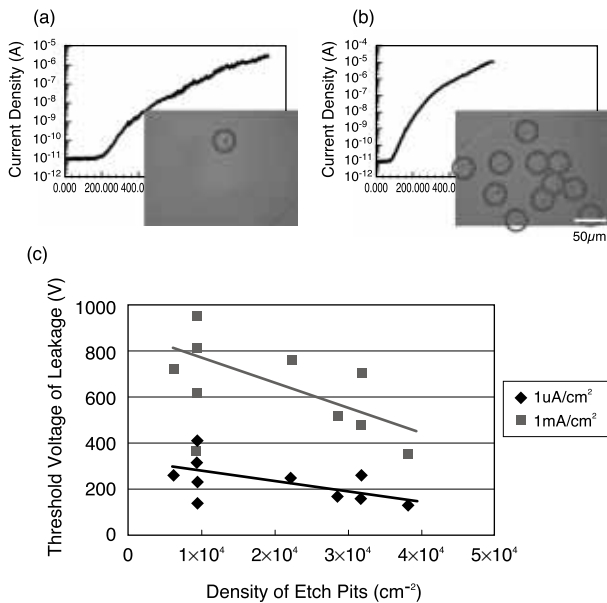


Fig. 17. Etch pit density and reverse characteristics of diamond SBD. (a) Leakage current was low at electrodes with low etch-pit density. (b) Leakage current was high at electrodes with high etch-pit density. (c) Threshold voltage of leakage current vs density of etch pits. Threshold voltage decreased as etch-pit density increased.

5. Conclusion

In this paper, diamond semiconductor technology was discussed through the development of diamond SBD. By growing a diamond epitaxial layer on a high off-angle substrate at a high microwave power, the formation of non-epitaxial crystallites were suppressed, and high mobility and extremely flat surface were achieved. After surface oxidization, the authors made a Pt Schottky diode having a high breakdown field of 3.1 MV/cm, which exceeds that of SiC. The reverse leakage current at high temperatures was three orders lower than that of SiC. The forward current density reached 3000 A/cm² at high temperatures. Both the forward and reverse characteristics of SBD after being heated for 1500 hours at 400 °C did not change, and high temperature stability was shown. The authors performed the diamond crystal defect study by using X-ray topography and the microwave etching method. This method revealed that mixed dislocations enhance the reverse leakage current of diamond SBD. This study revealed that diamond is the best material for devices that are energy saving, cooling free and high power density.

References

- (1) E.O. Johnson, RCA Rev., 2 (1965) 163
- (2) B.J. Baliga, J. Appl. Phys., 53 (1982) 1759
- (3) A.Q. Huang, IEEE Elec. Dev. Lett., 25 (2004) 298
- (4) H. Shiomi et al., Jpn. J. Appl. Phys., 29 (1990) L2163.
- (5) D.J. Twitchen et al., IEEE Trans. Elec. Dev., 51 (2004) 826.
- (6) T. Teraji et al., Appl. Surf. Sci., 254 (2008) 6273.
- (7) S.J.Rashid et al., IEEE Int'l Symposium on Power Semiconductor Devices, Proc.315, (2005)
- (8) S. Koizumi, K. Watanabe, M. Hasegawa and H. Kanda, Diam. Relat. Mater., 11 (2002) 307.
- (9) H. Kawarada et al., New Diam. Front. Carbon Technol., 17 (2007) 201
- (10) M. Kasu et al., Electron Lett., 41 (2005) 22.
- (11) H. Umezawa, T. Saito, N. Tokuda, M. Ogura, S. G. Ri, H. Yoshikawa, and S. Shikata, Appl Phys. Lett., 90, 073506 (2007)
- (12) N. Tatsumi, H. Umezawa, and S. Shikata, Int'l Conf. SiC and Related Materials, Proc. Th-99 (2007)
- (13) S. Shikata, H. Umezawa, N. Tatsumi, K. Ikeda and R. Kumaresan, 6th Conf. SiC and Related Wide Band-gap Materials, p.55 (2007)
- (14) T. Hatakeyama, T. Shinohe, Mater. Sci. Forum, 389, p.1169 (2002)
- (15) H. Umezawa, N. Tatsumi, K. Ikeda, R. Kumaresan and S. Shikata, 6th Conf. SiC and Related Wide Band-gap Materials, p.57 (2007)
- (16) J.-L. Robert et al., Sensors and Actuators A, 97-98 (2002) 27.
- (17) V. Saxena, J. N. Su, A. J. Steckl, IEEE Trans. Elec. Dev., 46, p.456 (1999)
- (18) S. Shikata, K. Ikeda, R. Kumaresan, H. Umezawa and N. Tatsumi, Materials Science Forum 617, (2009) 999-1002
- (19) K. Ikeda, H. Umezawa, K. Ramanujam, and S. Shikata, Appl. Phys. Express, 2, 011202 (2009)
- (20) Q. Wahab et al., Appl. Phys. Lett., 76 (2000) 2025.
- (21) N. Tatsumi, H. Umezawa, K. Ikeda, R. Kumaresan, Y. Nishibayashi, T. Imai, and S. Shikata, Int'l Conf. New Diamond and Nano Carbons., Proc. p234(2008)
- (22) N. Tatsumi, H. Umezawa, T. Kato, H. Yamaguchi, R. Kumaresan, Y. Nishibayashi, T. Imai and S. Shikata, 22 nd Diamond symposium, p.106 (2008)

~~~~~  
**Contributors** (The lead author is indicated by an asterisk (\*).)

**N. TATSUMI\***

- Electronics R&D Laboratories,  
He is engaged in the research of diamond electron emitters and diamond electronic devices.



**K. IKEDA**

- Ph. D., National Institute of Advanced Industrial Science and Technology, Diamond Research Center (Now the SEI Electronics R&D Laboratories)

**H. UMEZAWA**

- Dr. of Eng., Diamond Research Center, National Institute of Advanced Industrial Science and Technology

**S. SHIKATA**

- Dr. of Eng., Diamond Research Center, National Institute of Advanced Industrial Science and Technology